Articles

Conformational Analysis of Chirally Deuterated Tunicamycin as an Active Site Probe of UDP-*N*-Acetylhexosamine:Polyprenol-P *N*-Acetylhexosamine-1-P Translocases[†]

Lin Xu,[‡] Michael Appell,[§,ǁ] Scott Kennedy,[‡] Frank A. Momany,[§,ǁ] and Neil P. J. Price*,[‡,§,⊥]

USDA-ARS-NCAUR, Fermentation Biotechnology Research Unit, and Plant Polymer Research Unit, 1815 North University Street, Peoria, Illinois 61604, and University of Rochester Medical Center, 601 Elmwood Avenue, Rochester, New York 14642

ABSTRACT: Tunicamycins are potent inhibitors of UDP-*N*-acetyl-D-hexosamine:polyprenol-phosphate *N*-acetylhexosamine-1-phosphate translocases (D-HexNAc-1-P translocases), a family of enzymes involved in bacterial cell wall synthesis and eukaryotic protein N-glycosylation. Structurally, tunicamycins consist of an 11-carbon dialdose core sugar called tunicamine that is N-linked at C-1′ to uracil and O-linked at C-11′ to *N*-acetylglucosamine (GlcNAc). The C-11′ O-glycosidic linkage is highly unusual because it forms an α/β anomeric-to-anomeric linkage to the 1-position of the GlcNAc residue. We have assigned the ^{1}H and ^{13}C NMR spectra of tunicamycin and have undertaken a conformational analysis from rotating angle nuclear Overhauser effect (ROESY) data. In addition, chirally deuterated tunicamycins produced by fermentation of *Streptomyces chartreusis* on chemically synthesized, monodeuterated (*S*-6)-[^{2}H$_1$]glucose have been used to assign the geminal H-6′a, H-6′b methylene bridge of the 11-carbon dialdose sugar, tunicamine. The tunicamine residue is shown to assume pseudo-D-ribofuranose and ^{4}C$_1$ pseudo-D-galactopyranosaminyl ring conformers. Conformation about the C-6′ methylene bridge determines the relative orientation of these rings. The model predicts that tunicamycin forms a right-handed cupped structure, with the potential for divalent metal ion coordination at 5′-OH, 8′-OH, and the pseudogalactopyranosyl 7′-O ring oxygen. The formation of tunicamycin complexes with various divalent metal ions was confirmed experimentally by MALDI-TOF mass spectrometry. Our data support the hypothesis that tunicamycin is a structural analogue of the UDP-D-HexNAc substrate and is reversibly coordinated to the divalent metal cofactor in the D-HexNAc-1-P translocase active site.

Tunicamycin is a substrate analogue inhibitor for *N*-acetyl-D-hexosamine-1-phosphate translocases (MraY, WecA, WbcO, etc.), enzymes that catalyze the formation of HexNAc-PP-undecaprenol, the first step in the formation of several bacterial polysaccharides (*1−4*). In eukaryotes, the target translocase (known as GPT) catalyzes the biosynthesis of *N*-acetylglucosamine-linked dolichol pyrophosphate (*5, 6*), an early event in protein N-glycosylation, and tunicamycin is therefore widely used to inhibit glycoprotein translocation and processing. The translocases are integral membrane proteins, and only recently has a bacterial MraY protein been sufficiently overexpressed to enable its purification (*7*).

However, models of the membrane topology of MraY and WecA have been proposed on the basis of localization of FLAG and β-lactamase inserts, respectively (*8, 9*), and have been refined by comparative sequence alignment of the translocase superfamily (*10−13*). These studies indicate that the UDP-sugar binding site and the translocase active site are located on the five cytoplasmic loops located on the cytoplasmic side of the membrane. Two conserved aspartyl residues located in loop 2 (Asp116 and Asp117 for MRAY_ECOLI) are postulated to be part of a DDXXD motif necessary for binding Mg^{2+} cofactor (*14, 15*). A third conserved Asp (Asp267 for E_COLI MRAY) is located in an adjacent loop (*15*) or just within the cytoplasmic face of the transmembrane (TM) domain 8 (*12*). This has been implicated in a double displacement mechanism in which the HexNAc-1-P[1] is initially transferred from UDP-HexNAc to the TM-8 aspartyl group, with UMP as the leaving group, followed by transfer to undecaprenol phosphate.

* To whom correspondence should be addressed. E-mail: pricen@ncaur.usda.gov. Tel: (309) 681-6246. Fax: (309) 681-6427.

[‡] University of Rochester Medical Center.

[§] USDA-ARS-NCAUR.

[ǁ] Plant Polymer Research Unit.

[⊥] Fermentation Biotechnology Research Unit.

[1] Abbreviations: HexNAc, *N*-acetylhexosamine; GlcNAc, *N*-acetylglucosamine; MALDI-TOF, matrix-assisted laser desorption ionization−time of flight; MS, mass spectrometry; NMR, nuclear magnetic resonance.

The tunicamycins are streptomycetes-derived natural products that contain an 11-carbon dialdose sugar called tunicamine (16−18). One anomeric carbon of tunicamine (C-1′) is N-glycosidically linked to uracil, while the other (C-11′) is O-glycosidically linked to *N*-acetylglucosamine (GlcNAc). The tunicamine C-11′ O-glycosidic linkage is highly unusual because it is β-linked to the 1-position of the GlcNAc residue to form an α/β anomeric-to-anomeric linkage. The amino group at C-2 of the tunicamine is N-acylated with a variety of different fatty acids, and 17 different tunicamycins have been described (19). Kinetic studies with the bacterial translocase MraY indicate that tunicamycin is a reversible competitive inhibitor with respect to the sugar nucleotide substrate but is noncompetitive with regard to the polyprenol phosphate (15, 20). This suggests that tunicamycin competes with the UDP-HexNAc for binding at the active site but that prenol phosphate binding is distal. Naturally occurring UDP-sugars are generally α-linked with respect to the hexosamine residue, and to be an effective substrate analogue for this reaction, it is predicted that the 1″,11′-linked GlcNAc residue of tunicamycin should have an axial configuration about the C-1″ anomeric carbon. Hence, the O-linked GlcNAc residue of tunicamycin is assumed to mimic the HexNAc-1-phosphate transferred by the translocase enzyme, while the N-glycosidically linked uracil mimics the uracil of the UMP leaving group.

We have assigned the ^{1}H and ^{13}C NMR spectra of tunicamycin and have undertaken a conformational analysis from rotating angle nuclear Overhauser effect (ROESY) data. In addition, chirally deuterated tunicamycins produced by fermentation of *Streptomyces chartreusis* on chemically synthesized, monodeuterated (*S*-6)-[[2]H$_1$]glucose have been used to assign the geminal H-6′a, H-6′b methylene bridge of the 11-carbon dialdose sugar, tunicamine. The tunicamine residue is shown to assume pseudo-D-ribofuranose and [4]C$_1$ pseudo-D-galactopyranose ring conformers. The conformation about the C-6′ methylene bridge determines the relative orientation of these rings. Also considered are (i) the spatial relationship of the uracil ring to the pseudoribosyl moiety, (ii) conformation and anomericity of the 1′,11″-glycosidic bonds, and (iii) the spatial arrangement of the N-linked acyl chain with respect to the carbohydrate moiety. Our data support the hypothesis that tunicamycin is a structural analogue of the UDP-D-HexNAc substrate and is reversibly coordinated to the divalent metal cofactor, Mg^{2+}, in the D-HexNAc-1-P translocase active site. Tunicamycin, therefore, prevents UDP-HexNAc binding to the translocases by occupying its coordination sites to the Mg^{2+} cofactor.

MATERIALS AND METHODS

Tunicamycin was obtained by methanol extraction from mycelia of *S. chartreusis* NRRL 3882 (18) or obtained commercially from Sigma Chemicals. *S. chartreuses* strains were maintained and cultured on TYD medium as described previously (18). Chirally deuterated (6-*S*)-[[2]H$_1$]glucose was synthesized from [6,6′-[2]H$_2$]glucose as described previously (21). Chirally labeled tunicamycin was extracted and purified from *S. chartreusis* cultured on TYD medium in which the dextrose was replaced with (6-*S*)-[[2]H$_1$]glucose. Isotopic enrichments were confirmed by various nuclear magnetic resonance (NMR) experiments as described below and by electrospray LC-MS (19).

NMR Spectroscopy. Standard and metabolically labeled tunicamycins were deuterium-exchanged by lyophilization from D$_2$O and redissolved in deuterated methanol. Spectra were recorded on a Bruker Avance 600 MHz instrument using pulse sequences supplied by Bruker. HSQC spectra were obtained using Echo/Antiecho-TPPI utilizing gradient selection with decoupling during acquisition. Additional spectra of the chirally deuterated tunicamycin were obtained in deuterated methanol on a Varian Unity INOVA 600.
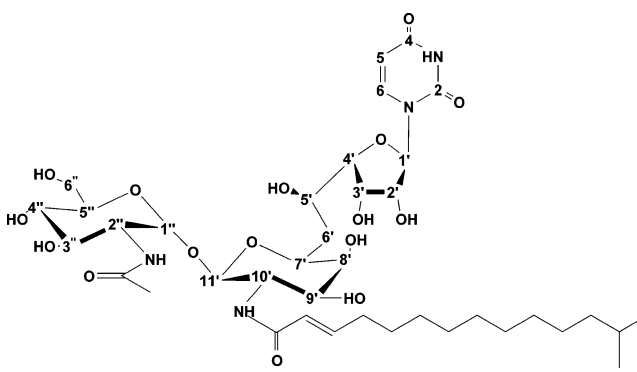
Matrix-Assisted Laser Desorption Ionization−Time-of-Flight (MALDI-TOF) Mass Spectrometry and Binding of Divalent Metal Ions. MALDI-TOF mass spectra were recorded on a Bruker-Daltonic Omniflex instrument operating in reflecton mode. Ion source 1 was set to 19.0 kV and source 2 to 14.0 kV, with lens and reflector voltages of 9.20 and 20.00 kV, respectively. A 200 ns pulsed ion extraction was used with matrix suppression up to 400 Da. Excitation was at 337.1 nm, typically at 60% of 150 μJ maximum output, and 80 shots were accumulated. Tunicamycin (10 μL, 2.5 mg·mL^{-1} in methanol) was mixed with 2,5-dihydrobenzoic acid matrix (10 μL; saturated in acetonitrile) and the appropriate divalent metal ion salt (10 μL; 5% w/v in water). Samples were dried under a lamp on a conventional 7 × 7 target. The instrument was calibrated externally on a dp series of maltooligosaccharides.

Molecular Modeling. Molecular modeling with mechanics and dynamics simulations was carried out using InsightII (2000.3L)/Discover (Accelrys Inc., San Diego, CA). Energy calculations were carried out using an in-house modified AMBER force field, similar to that described previously (22) within the Discover program. In all empirical calculations the dielectric constant is treated as $\epsilon = 1$ with the nonbonded 1−4 terms scaled by 0.75. Carbohydrate charges were taken from previous work on amylose fragments (23) while the uracil was given charges through the charging mechanism in AMBER. Density functional calculations were carried out using the Parallel Quantum Solutions (PQS) software (v3.1) and hardware (24). Energy minimization calculations were carried out at the B3LYP/6-311++G** level of theory to achieve correct geometry for the carbohydrate moieties.

RESULTS AND DISCUSSION

(i) Conformation and Anomericity Proximal to the $\alpha\beta$-1″,11′-Glycosidic Bond. The NMR spectrum of tunicamycin is characterized by four independent spin systems: the N-linked uracil ring, the tunicamine 11-carbon sugar system, the α1″,11′-linked *N*-acetylglucosaminyl residue, and the N-linked acyl group (Table 1). Controversy exists as to which of the tunicamycin 1″,11′-O-glycosidic linkages is α and β, and assignments based on low-field NMR and circular dichroism data (16) have been called into question by a high-field PMR analysis of the tunicamycin-like corynetoxins (25). Because the UDP-*N*-acetylhexosamine sugar nucleotides are typically α-O-linked (26, 27), the *O*-GlcNAc residue of tunicamycin is predicted to be α-linked, thereby mimicking the HexNAc-1-P transferred by the translocase enzymes.

The anomeric-to-anomeric 1″,11′-O-glycosidic protons are evident from the axial doublet of the β-anomer at 4.71 ppm ($J_{10',11'} = 3.48$ Hz) and the equatorial α-anomeric doublet at 5.04 ppm ($J_{1″,2″} = 8.44$ Hz). The tunicaminyl and *O*-GlcNAc ring protons were assigned from a time-resolved 1-D TOCSY

Table 1: Assignment of ^{13}C and Proton NMR Chemical Shifts[a]

	tunicamycin assignments				uridine assignments			
structural motif	carbon residue	C13 shift assigned	proton residue	H1 shift assigned	carbon residue	C13 shift assigned	proton residue	H1 shift assigned
uracil	C-2	152.62[c]			C-2	151.89[c]		
	C-4	166.12[c]			C-4	166.43[c]		
	C-5	103.06	H-5	5.89 (d)	C-5	102.62	H-5	5.79 (d)
	C-6	142.76	H-6	8.05 (d)	C-6	142.20	H-6	7.77 (d)
tunicamine/ribose	C-1′	89.89	H-1′	6.05 (d)	C-1′	89.75	H-1′	5.80 (d)
	C-2′	75.48	H-2′	4.31 (t)	C-2′	74.06	H-2′	4.24 (t)
	C-3′	70.87	H-3′	4.34 (dd)	C-3′	69.78	H-3′	4.12 (t)
	C-4′	89.61	H-4′	3.96 (d)	C-4′	84.56	H-4′	4.03 (m)
	C-5′	68.36	H-5′	4.12 (t)	C-5′	61.10[b]	H-5′a/b	3.81/3.70
	C-6′	35.93[b]	H-6′a/b	2.20/1.63				
	C-7′	72.59	H-7′	3.91 (t)				
	C-8′	72.06	H-8′	3.78 (s)				
	C-9′	73.31	H-9′	3.78 (s)				
	C-10′	54.46	H-10′	4.19 (t)				
	C-11′	101.99	H-11′	4.71 (d)				
GlcNAc	C-1″	100.28	H-1″	5.04 (d)				
	C-2″	54.92	H-2″	3.98 (dd)				
	C-3″	72.79	H-3″	3.80 (t)				
	C-4″	72.46	H-4″	3.48 (t)				
	C-5″	74.30	H-5″	4.11 (t)				
	C-6″	63.17[b]	H-6″a/b	3.93/3.82				
	C=O	173.49[c]						
	CH$_3$	23.23	CH$_3$	2.05 (s)				
N-acyl chain	C=O	169.73[c]						
	C-2‴	124.94	H-2‴	6.07 (d)				
	C-3‴	146.49	H-3‴	6.94 (dt)				
	C-4‴	33.05[b]	H-4‴	2.32 (m)				
	C-5‴	29.47	H-5‴	1.58 (m)				
	(CH$_2$)$_n$	30−31[b]	(CH$_2$)$_n$	1.40 (s)				
	ω-CH$_2$	40.25	ω-CH$_2$	1.26 (m)				
	CH	29.15	CH	1.57 (m)				
	CH$_3$'s	23.02	CH$_3$'s	1.00/0.99				

[a] The numbering is referenced above. [b] Confirmed by a DEPT experiment. [c] Confirmed from HMBC data.

experiment (Figure 1, left). Correlations are observed from the GlcNAc equatorial H-1″ at 5.04 ppm through H-2″eq, H-3″eq, H-4″eq, and H-5″eq and subsequently to H-6″a. From the tunicamine axial anomeric proton H-11′ correlations were observed to H-10′ax (4.19 ppm, t) and H-9′ax (3.78 ppm, d), but no correlation was observed between the axial H-9′ and the equatorial H-8′. This small $J_{8',9'}$ equatorial−axial coupling established the *galacto* configuration of the tunicamine pseudopyranosyl ring. By contrast, coupling between the corresponding H-3″ax and H-4″ax protons of the *O*-GlcNAc residue gave the expected TOCSY correlation ($J_{3'',4''}$ = 9.54 Hz), thereby confirming the anomericity and *gluco* configuration of the α-linked sugar. These data indicate that the 11-carbon tunicamine sugar assumes two hemiacetal ring closures that result in the pseudo-D-ribofuranose 5-carbon ring and a pseudo-D-galactopyranosamine 6-carbon ring.

Protons H-3′ and H-2′, H-5′ and H-5″, and especially the cluster of H-3″, H6″b, H-8′, and H-9′ signals were incompletely resolved in the proton NMR spectrum but were readily assigned from a HSQC heteronuclear correlation experiment (Figure 2). Further assignments were made from COSY, ROESY, and 2-D TOCSY data of the anomeric region (Figure 1, right). COSY cross-peaks from H-1″ and H-11′ assigned H-2″ and H-10′, respectively. Data from the 2-D TOCSY (Figure 1, right) confirmed the result of the 1-D TOCSY experiment (Figure 1, left) and assigned H-1″, H-2″, H-3″, H-4″, H-5″ and H-11′, H-10′, H-9′ as coupled spin systems. The ROESY through-space correlation from H-11′ to H-1″ is absent from the TOCSY and COSY and confirms the presence of the 1″-axial to 11′-equatorial anomeric-to-anomeric O-glycosidic attachment. In addition, a small ROESY correlation occurs between GlcNAc H-1″
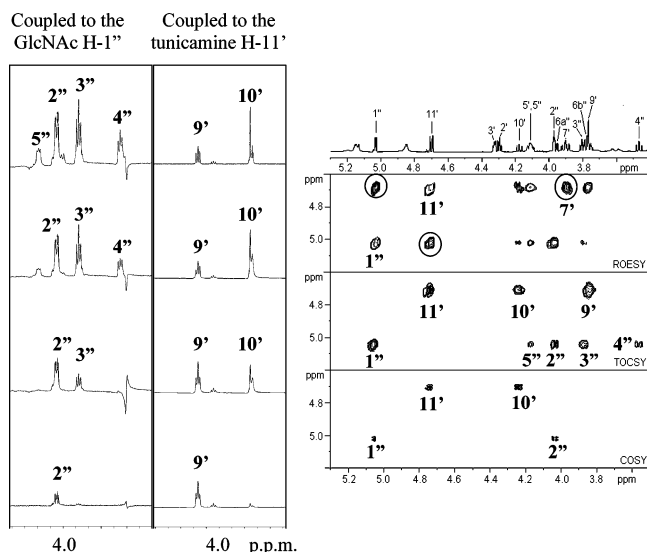
FIGURE 1: Correlation NMR data. (Left) Time-resolved 1-D TOCSY. Assignment of the carbohydrate ring protons coupled to the 1″,11′-anomeric protons, GlcNAc α-1″ and tunicamine β-11′. Small $J_{8',9'}$ results from the equatorial H-8′, evidence for the pseudogalactopyranosyl ring conformation of C6′−C11′. The correlations from H1″ to H5″ are assigned to the α-GlcNAc residue. (Right) Correlation NMR (COSY, TOCSY, ROESY) of the carbohydrate ring protons. Tunicamine (11′, 10′, 9′) and GlcNAc (1″−5″) couplings are evident. Through-space coupling occurs across the α,β-1″,11′-anomeric linkage (circled) and from H-11′ to H-7′ (circled).

to the tunicaminyl H-10′ (equatorial to axial, through-space) but not from H-11′ to H-2″ (axial to axial). The relative intensity of the H-1″−H-11′ (strong) and H-1″−H-10′ (weak) through-space couplings suggests that the *N*-acyl and *N*-acetyl groups are orientated to the same side of the tunicamycin molecule but on the opposite side to the pseudoribosyl moiety (Figure 5). Through-space ROESY couplings also indicate that the six tunicamine carbons (C-6′ through C-11′) of the pseudogalactopyranosaminyl ring form a $^4C_1$ chair configuration (Figure 5). This is evident from the ROESY correlations from the anomeric H-11′ axial proton to H-7′ (axial) and to H-9′ (axial) (Figure 1, right). The lack of a TOCSY correlation to the equatorial H-8′ proton (Figure 1) confirmed the *galacto* configuration of the pseudopyranosaminyl ring.

An HMBC three-bond correlation is observed across the glycosidic oxygen from the tunicaminyl β-11′ proton to the α-D-GlcNAc-1″ carbon, confirming the ROESY H-1″−H-11′ through-space correlation (Figure 1). The reciprocal H-1″−C-11′ HMBC correlation is not observed, but two-bond H-1″−C-2″ and three-bond H-1″−C-3″ correlations are present. These latter assignments were confirmed by HMBC $^{13}C−^1H$ correlations from the well-resolved GlcNAc H-4″ and carbons C-2″ and C-3″ and to the methylene C-6″ bridge carbon which was assigned by an inverse HMQC-DEPT signal (Figure 2). Taken together, these data demonstrate that the tunicaminyl 11′-anomeric linkage is β, with the D-GlcNAc residue α-linked, and the C-6′−C-11′ of the tunicamine dialdose assumes a pseudogalactopyranose $^4C_1$ chair.

(ii) Spatial Relationship of the N-Uracil to the Pseudoribofuranosyl Ring. Four carbonyl groups were deduced from the ^{13}C NMR spectrum of tunicamycin, one from each of the *N*-acyl groups and two from the uracil ring. These were
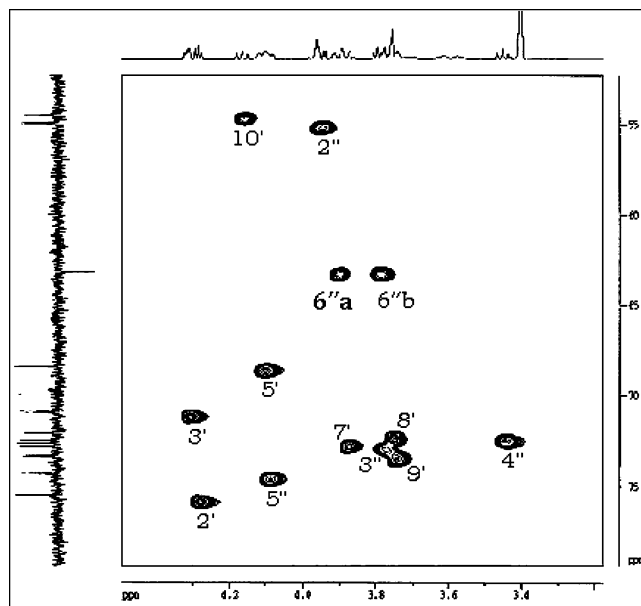

FIGURE 2: $^{13}C−^1H$ heteronuclear HSQC and ^{13}C phase-transfer DEPT spectra of the carbohydrate ring protons. Note the resolution of the 2′ and 3′ signals, and 5′ and 5″, which are poorly resolved in the proton spectrum. Methylene protons H-6″a and H-6″b correlate to a negative DEPT signal for C-6″ at 63.7 ppm.
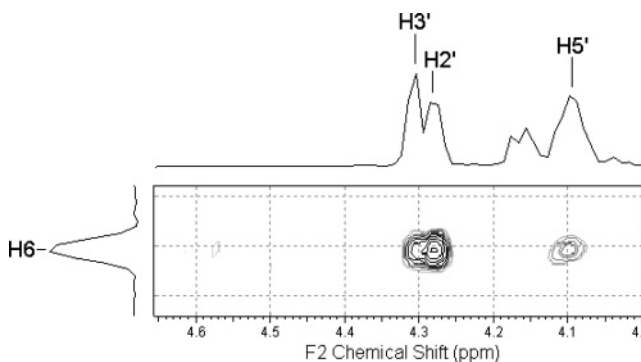

FIGURE 3: ROESY through-space correlations from the *N*-uracil H-6 at 8.05 ppm to the tunicamine protons H-2′, H-3′, and H-5′. This determines the *anti* conformation of the uracil group and the *exo*-2′-*endo*-3′ ring pucker of the pseudo-D-ribofuranosyl ring.

assigned from HMBC long-range couplings. Uracil proton H-6 (8.05 ppm) shows two-bond coupling to C-5 and three-bond coupling to the tunicaminyl N-linked anomeric carbon C-1′ and to both C-4 and C-6 ring carbonyls. Similarly, uracil H-5 couples to C-6 and displays a weak HMBC two-bond correlation to its sole neighboring carbonyl, C-4. In addition, three-bond coupling is apparent between the H-1′ pseudoribosyl anomeric proton and the uracil C-2 carbonyl. These correlations define the assignments for the *N*-uracil ring. The N-glycosidic anomeric proton of the pseudoribosyl ring (H-1′) is evident at 6.05 ppm. This shows a COSY cross-peak to the H-2′ triplet (4.31 ppm, $J_{1',2'} = 11$ Hz), with the large coupling constant indicating that the uracil is in an equatorial configuration.

The uracil H-5 and H-6 assignments are confirmed by their observed TOCSY, COSY, and ROESY correlations. Further ROESY through-space correlations were apparent between H-6 of the uracil ring and H-2′, H-3′, and H-5′ of the pseudoribofuranosyl moiety (Figure 3). The strongest of these through-space correlations is between the uracil H-6 and the tunicamine H-2′. These assignments, particularly the H-5′
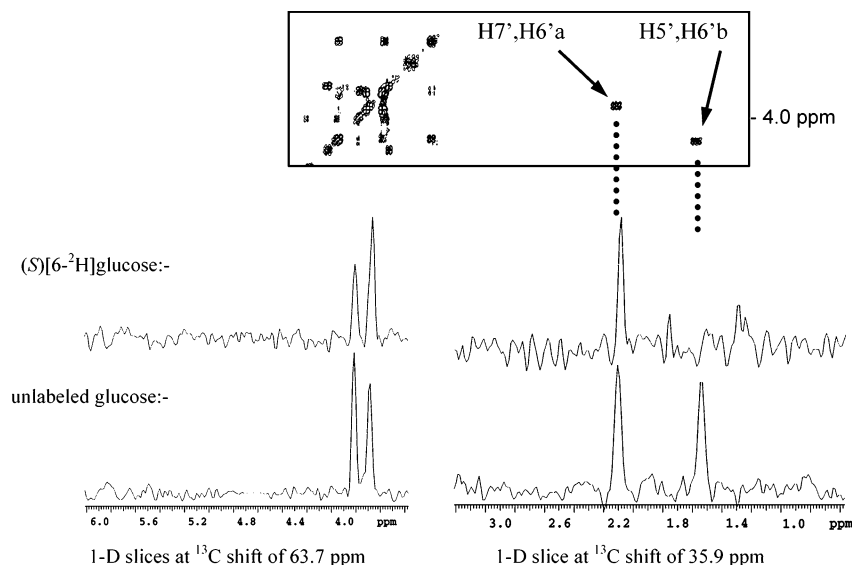
FIGURE 4: Assignment of the tunicamine 6′-methylene protons. (Top) Detail of the COSY correlations for unlabeled tunicamycin from H-5′ and H-7′ to the methylene bridge *gem* protons H-6′a (2.20 ppm) and H-6′b (1.63 ppm). The correlations from H-5′−H-6′a and H-7′−H-6′b are precluded due to unfavorable dihedral angles. (Bottom) 1-D slices along the HSQC ^{13}C axis of chirally deuterated tunicamycin obtained by fermentation of *S. chartreusis* on (S-6)-(^{1}H$_2$)glucose. The ^{13}C chemical shifts at 63.7 and 35.9 ppm are for the 6″-C and 6′-C methylene carbons, respectively. The tunicamine geminal proton H-6′b (1.63 ppm), coupled to H-5′, is selectively deuterated, resulting in the loss of its proton signal. The tunicamine H-6′a (2.20 ppm) and the α-GlcNAc geminals, H-6″a and H-6″b, are unaffected. The control tunicamycin was from *S. chartreusis* grown on unlabeled glucose.

to H-6 correlation, therefore suggest that the pseudoribosyl moiety of tunicamycin has a D-ribofuranoside configuration. The proximity of the H-6 proton to H-2′ indicates that the 5,6 double bond of the uracil ring has *anti* orientation with respect to the pseudoribosyl ring, with the pseudoribofuranose in an *endo-2′-exo-3′* puckered conformation. This N-glycosidic linkage of the pseudoribosyl ring to uracil in *anti* conformation is therefore a close structural analogue of the uridylyl motif of the translocase-catalyzed UMP leaving group.

(iii) Spatial Arrangement of the N-Linked Acyl Chain with Respect to the Tunicaminyl Moiety. TOCSY and COSY correlations arising from the *N*-acyl spin system indicate the presence of the αβ-*trans* double bond and also assigned the H-4‴ and H-5‴ acyl methylene protons. Long-range HMBC correlations from the acyl carbonyl carbons further assigned the *N*-acyl and *N*-acetyl groups. Hence, the tunicaminyl H-10′ exhibits three-bond ^{13}C−^{1}H coupling to the fatty acid C-1‴ carbonyl. The latter also has a two-bond ^{13}C−^{1}H coupling to the fatty acid α-proton (H-2‴) at 6.07 ppm and a three-bond coupling to the fatty acid H-3‴ (6.94 ppm). Similarly, the GlcNAc *N*-acetyl carbonyl is three-bond coupled to the GlcNAc H-2″ proton (3.98 ppm) and two-bond coupled to the acetyl methyl protons at 2.05 ppm. These data are further confirmed by the HSQC and COSY spectra. However, although there are ROESY correlations from H-2‴ and H-3‴ to the H-4‴ methylene protons (2.32 ppm), further through-space coupling to the H-5‴ or the chain methylenes is not observed. This suggested that the *N*-acyl group is essentially fully extended during the time course of the experiment and does not fold back to within NOE contact distance either with itself or with the tunicaminyluracil part of the molecule.

(iv) Spatial Relationships about the Tunicamine 5′, 6′, 7′ Methylene Bridge. The conformation at the 4′-, 5′-, 6′-, and 7′-positions of the tunicamine motif dictates the spatial relationship of the pseudogalactopyranosyl ring with respect to the pseudoribofuranosyl ring. This was particularly

relevant because H-4′ and H-7′ are locked into ring configurations, so that free rotation is limited. By analogy with the transition state for the HexNAc-1-P translocases for the formation of the acyl-enzyme intermediate, these tunicamine 4′, 5′, 6′, 7′ conformational data were expected to provide insight into the facial stereochemistry of the UMP leaving group. From DEPT and HMQC data, two carbohydrate methylenes were assigned for tunicamycin. The GlcNAc 6″-position gives rise to a C-6″ carbon signal at 63.17 ppm and H-6″ proton signals at 3.93 and 3.82 ppm. The tunicamine bridge methylene, C-6′, is apparent at 35.93 ppm, with the H-6′ geminal protons at 2.20 and 1.63 ppm. TOCSY and ROESY correlations were seen from the H-6′ geminals to H-5′ and H-7′, but in the COSY spectrum only H-6′a−H-7′ and H-5′−H-6′b correlations were observed (Figure 4, top). This is attributed to small $J_{6′b,7}$ and $J_{5,6′a}$ coupling constants, an indicator that the H-6′b−H-7′ and H-5′−H6′b dihedral angles approach +90° or −90°. In addition, COSY showed that the pseudoribosyl H-5′ and H-4′ coupling was also small, indicating that these protons also approached 90°. The H-5′ hydroxyl group of natural tunicamycin is in the *R* configuration, and synthetic *epi*-tunicamycin (i.e., *S*-5′-OH) is known to be less effective as an inhibitor of HexNAc-1-P translocase (*28*). MraY translocase is also inhibited by mureidomycin and liposidomycin (*29, 30*), and SARS studies on synthetic analogues of these inhibitors also stress the requirement for a defined chiral hydroxyl group which corresponds to the tunicamycin 5′-OH (*31−33*). The chirality of the 5′-OH group is therefore crucial to inhibitory activity and, as discussed below, is correctly positioned to form a ligand to the Mg^{2+} cofactor in the HexNAc-1-P translocase active site.

To conclusively assign the H-6′a and H-6′b geminal protons, and to confirm the observed COSY correlations, required the preparation of tunicamycin that was chirally monodeuterated at the 6′-position. This was done by culturing *S. chartreuses* on synthetically prepared (*S*)-[6-^{2}H$_1$]glucose
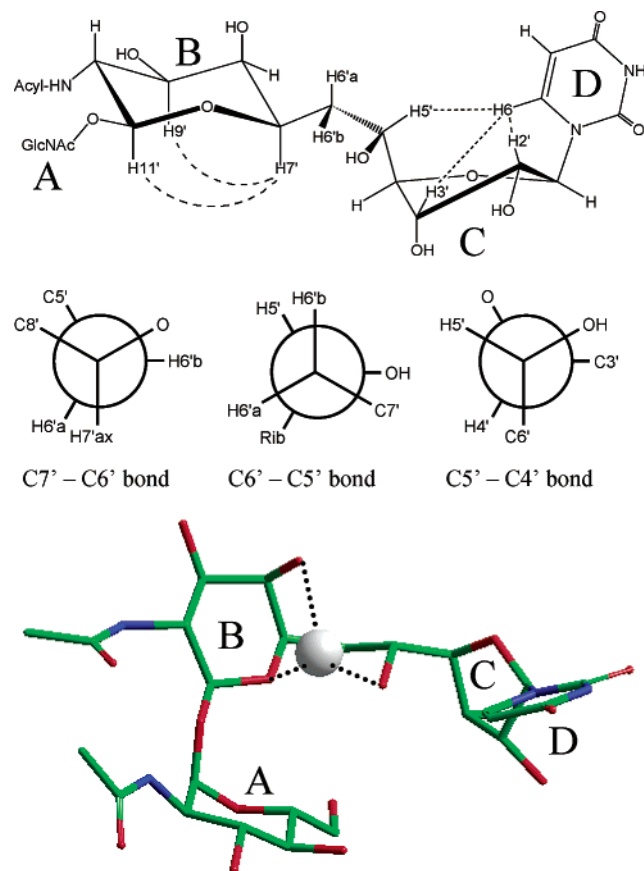
FIGURE 5: Conformational model for tunicamycin. (Top) The 11-carbon dialdose, tunicamine, assumes pseudo-D-galactopyranose (B ring) and pseudo-D-ribofuranose (C ring), with a C-5′(+), C-6′-(+), C-7′(+) bridge conformation. The uracil (D ring) is *anti* aligned and the *N*-acyl groups are extended from the back face. ROESY though-space correlations are indicated by broken lines. (Center) Newman projects of the C-7′−C-6′, C-6′−C-5′, and C-5′−C-4′ bonds consistent with the observed NMR data. (Bottom) Conformational model for tunicamycin. This arrangement facilitates chelation of divalent metal ion to 5′-OH, 8′-OH, and the $^4C_1$ pseudogalactopyranosyl ring oxygen.

as a sole carbon source. The labeled tunicamycin was recovered as described previously and subjected to HSQC and COSY correlation analysis. One-dimensional slices were taken along the HSQC ^{13}C axis at 63.7 ppm (i.e., GlcNAc C-6″) and at 35.9 ppm (tunicamine C-6′) in order to visualize the coupled geminal protons (Figure 4, bottom). The tunicamine geminal H-6′b signal at 1.63 ppm was absent for the labeled tunicamycin, evidence that it had become selectively deuterated. The tunicamine H-6′a (2.20 ppm) and the *O*-GlcNAc geminals, H-6″a and H-6″b, were unaffected (Figure 4). This was also apparent in the COSY spectrum by the lack of the H−H cross-peak from H-5′ to the deuterated H-6′b (data not shown). Hence these data assigned the absolute stereochemistry of the H-6′a and H-6′b protons and clearly demonstrated that H-6′a was selectively coupled to H-7′, but not H-5′, and that H-6′b was coupled to H-5′, but not H-7′.

From these data it is possible to propose a structural model where the tunicamine assumes a 5′(+), 6′(+), 7′(+) conformation, with the uracil *anti* aligned and the *N*-acetyl and *N*-acyl chain extended from the back face (Figure 5). Consistent with the ROESY data (Figure 3), this model places the uracil H-6 proton 2.91 Å from H-5′, and 3.58 Å

from H-2′. This is also consistent with intramolecular hydrogen bonding between the pseudoribosyl 2′-OH and the uracil 2-O carbonyl. A weaker ROESY correlation is also observed for uracil H-6 to H-3′ (Figure 3), but the in vacuo calculated distance is 4.85 Å, presumably due to solvation effects. These data confirm the *anti* conformation of the uracil group and the *exo*-2′-*endo*-3′ ring pucker of the pseudo-D-ribofuranosyl ring (Figure 5). The bridge between the pseudoribofuranose (C ring) and pseudogalactopyranose (B ring) assumes a 5′(+), 6′(+), 7′(+) conformation, with the B ring in a $^4C_1$ chair. This places the tunicamine (*R*)-5′-OH oxygen almost equidistant from the pseudogalactosyl ring oxygen (7′-O) and the 8′-OH oxygen. These distances are 2.75 and 2.79 Å, respectively, with the distance across the pseudogalactosyl ring from 7′-O to 8′-O calculated at 2.99 Å. This arrangement facilitates chelation of divalent metal ions to 5′-OH, 8′-OH, and the pseudogalactosyl ring oxygen, with the metal ion presumed to be slightly out of plane. The GlcNAc and tunicamine anomeric protons, αH-1″ and βH-11′, are 2.32 Å apart in the model, in agreement with the strong through-space coupling observed in the ROESY spectrum (Figure 1) and in excellent agreement with an X-ray structure of α,β-trehalose (*34*). The calculated dihedral angles across the O-glycosidic linkage, H-11′−C-11′−O−C-1″ and H-1″−C-1″−O−C-11″, are 17.4° and 54.6°, respectively. This system is not perturbed by any intramolecular hydrogen bonding between the A ring and B, C, or D rings.

(v) Binding to Divalent Metal Ions. A model has been proposed for the active site of the MraY translocase in which Asp115 and Asp116 are coordinated to Mg^{2+}, which in turn is coordinated to the pyrophosphate bridge of the sugar nucleotide substrate. Our model predicts that tunicamycin is a close structural analogue of the UDP-sugar nucleotide substrate, where the 5′-OH, 8′-OH, and the pseudogalactosyl ring oxygen provide a structural mimic of the pyrophosphate bridge. Tunicamycin assumes a 5′(+), 6′(+), 7′(+) conformation, with the uracil *anti* aligned and the *N*-acyl chains extended from the back face. This arrangement facilitates chelation of divalent metal ions to the 5′-OH, 8′-OH, and the pseudogalactosyl ring oxygen. Hence, tunicamycin may bind to the D-HexNAc translocase enzymes by coordinating to the active site Mg^{2+} cofactor so that the DDXXD aspartyl residues occupy two coordination positions, with the tunicamycin 5′-OH, 8′-OH, and pseudogalactosyl ring oxygen occupying the other positions. Tunicamycin therefore prevents the binding of the UDP-sugar nucleotide by occupying its coordination sites to the Mg^{2+} cofactor.

To test this hypothesis, MALDI-TOF mass spectra were obtained on tunicamycin doped with various divalent metal ions (Figure 6, Table 2). In positive ion mode, Na^+ and K^+ adducts were observed for tunicamycins Tun-15, Tun-16, and Tun-17. These were separated by 14 mass units due to increasing size of the tunicamycin N-linked fatty acid (15, 16, and 17 carbons, respectively). Sodium adducts were also observed in the presence of the divalent metal ion and were accompanied by the expected metal adducts, i.e., [Tun + Mg]$^+$, [Tun + Mn]$^+$, [Tun + Cu]$^+$, and [Tun + Co]$^+$. Chelated divalent metal adducts of the type [Tun + M_2]$^+$ were observed, with one metal adducted as a counterion and the second complexed to the tunicamycin in the form of a metal chelate. Higher [Tun$_2$ + M]$^+$ and [Tun$_2$ + M_2]$^+$ ions were observed in the presence of Mg^{2+}, Mn^{2+}, or Co^{2+},
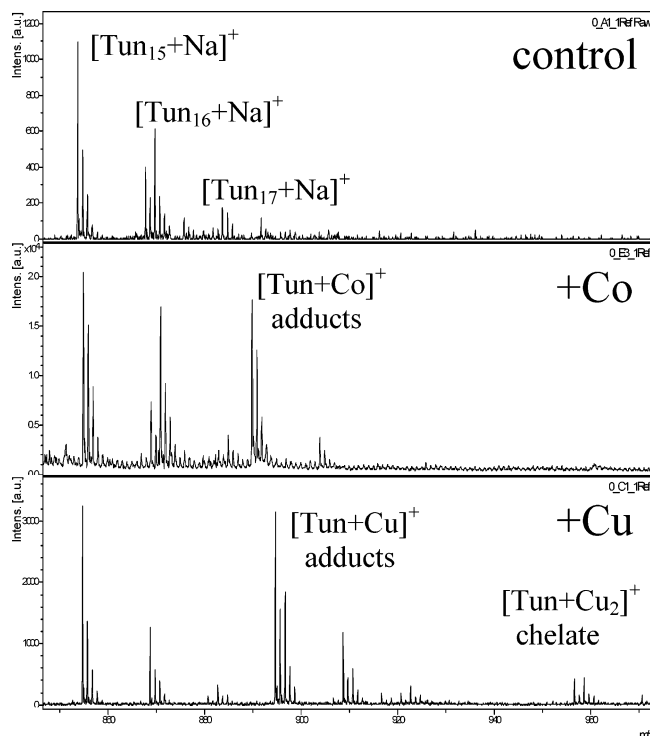
FIGURE 6: Tunicamycin chelation of divalent metal ions. MALDI-TOF mass spectra were obtained on tunicamycin in the absence of divalent metal ions (top) or in the presence of 5% metal salts. Tunicamycin *N*-acyl variants Tun15:1, Tun16:1, Tun16:0, and Tun17:0 are evident as sodium adducts at m/z 859, 875, 873, and 889, respectively. Cobalt and copper adducts [Tun15:1 + ^{63}Cu]$^+$ (m/z 899), [Tun15:1 + ^{65}Cu]$^+$ (m/z 901), and [Tun14:1 + ^{63}Cu]$^+$ (m/z 913) and [Tun15:1 + ^{59}Co]$^+$ (m/z 894), and [Tun14:1 + ^{59}Co]$^+$ (m/z 908) are observed. Tunicamycin−copper chelate ion (i.e., [Tun15:1 + ^{63}Cu$_2$]$^+$) is evident at m/z 962. Other assignments are reported in Table 2.

Table 2: Tunicamycin−Transition Metal Complexes Detected by Matrix-Assisted Laser Desorption Ionization−Time-of-Flight Mass Spectrometry (MALDI-TOF)[a]

metal ion	observed MS adducts
Na$^+$	[Tun + Na]$^+$
K$^+$	[Tun + K]$^+$
Cu^{2+}	[Tun + Cu]$^+$, [Tun + Cu$_2$]$^+$
Mg^{2+}	[Tun + Mg]$^+$, [Tun$_2$ + Mg]$^+$, [Tun$_2$ + Mg$_2$]$^+$
Mn^{2+}	[Tun + Mn]$^+$, [Tun$_2$ + Mn]$^+$, [Tun$_2$ + Mn$_2$]$^+$
Co^{2+}	[Tun + Co]$^+$, [Tun + Co$_2$]$^+$, [Tun$_2$ + Co]$^+$, [Tun$_2$ + Co$_2$]$^+$

[a] Spectra were obtained on tunicamycin in the presence of 5% divalent metal salts.

indicating the tunicamycin can form chelation dimers, with two tunicamycin molecules coordinated to one or two metal ions. These data support the hypothesis that tunicamycin inhibits D-HexNAc translocases by coordinating to the Mg^{2+} cofactor adjacent to the active site Asp-Asp motif.

Data presented in this paper indicate that tunicamycins target the translocase active site, potentially by forming ligands to the Mg^{2+} cofactor coordinated to the loop 2 conserved Asp-Asp motif. Hence, tunicamycin competitively inhibits the first step of the translocase bi-bi mechanism by inhibiting the binding of the sugar nucleotide substrate. An understanding of the architecture of the D-HexNAc translocase active site will help to elucidate the mechanism for their sugar nucleotide substrate specificity and may ultimately provide new target antibiotics directed against specific D-HexNAc translocase family members.

REFERENCES

1. Yamamori, S., Murazumi, N., Araki, Y., and Ito, E. (1978) Formation and function of *N*-acetyloglucosamine-linked phosphoryl- and pyrophosphorylundecaprenols in membranes from *Bacillus cereus*, *J. Biol. Chem. 253*, 6516−6522.
2. Barr, K., and Rick, P. D. (1987) Biosynthesis of enterobacterial common antigen in *Escherichia coli*. *In vitro* synthesis of lipid-linked intermediates, *J. Biol. Chem. 262*, 7142−7150.
3. Van Heijenoort, J. (2001) Formation of the glycan chains in the synthesis of bacterial peptidoglycan, *Glycobiology 11*, 25−36.
4. Rocchetta, H. L., Burrows, L. L., Pacan, J. C., and Lam, J. S. (1998) Three rhamnosyltransferases responsible for assembly of the A-band D-rhamnan polysaccharide in *Pseudomonas aeruginosa*: a fourth transferase, WbpL, is required for the initiation of both A-band and B-band lipopolysaccharide synthesis, *Mol. Microbiol. 28*, 1103−1119.
5. Scocca, J. R., and Krag, S. S. (1997) Aspartic acid 252 and asparagine 185 are essential for activity of lipid *N*-acetylglucosaminyl-phosphate transferase, *Glycobiology 7*, 1181−1191.
6. Zeng, Y., and Elbein, A. D. (1995) UDP-*N*-acetylglucosamine: dolichyl-phosphate *N*-acetylglucosamine-1-phosphate transferase is amplified in tunicamycin-resistant soybean cells, *Eur. J. Biochem. 233*, 458−466.
7. Bouhss, A., Crouvoisier, M., Blanot, D., and Mengin-Lecreulx, D. (2004) Purification and characterization of the bacterial MraY translocase catalyzing the first membrane step of peptidoglycan biosynthesis, *J. Biol. Chem. 279*, 29974−29980.
8. Amer, A. O., and Valvano, M. A. (2000) The *N*-terminal region of the *Escherichia coli* WecA (Rfe) protein, containing three predicted transmembrane helices, is required for function but not for membrane insertion, *J. Bacteriol. 182*, 498−503.
9. Bouhss, A., Mengin-Lecreulx, D., Le Beller, D., and Van Heijenoort, J. (1999) Topological analysis of the MraY protein catalysing the first membrane step of peptidoglycan synthesis, *Mol. Microbiol. 34*, 576−585.
10. Lehrman, M. A. (1994) A family of UDP-GlcNAc/MurNAc: polyisoprenol-P GlcNAc/MurNAc-1-P transferases, *Glycobiology 4*, 768−771.
11. Dal Nogare, A. R., Dan, N., and Lehrman, M. A. (1998) Conserved sequences in enzymes of the UDP-GlcNAc/MurNAc family are essential in hamster UDP-GlcNAc:dolichol-P GlcNAc-1-P transferase, *Glycobiology 8*, 625−632.
12. Anderson, M. S., Eveland, S. S., and Price, N. P. J (2000) Conserved cytoplasmic motifs that distinguish sub-groups of the polyprenol phosphate:*N*-acetylhexosamine-1-phosphate transferase family, *FEMS Microbiol. Lett. 191*, 169−175.
13. Amer, A. O., and Valvano, M. A. (2001) Conserved amino acid residues found in a predicted cytosolic domain of the lipopolysaccharide biosynthetic protein WecA are implicated in the recognition of UDP-*N*-acetylglucosamine, *Microbiology 147*, 3015−3025.
14. Amer, A. O., and Valvano, M. A. (2002) Conserved aspartic acids are essential for the enzymic activity of the WecA protein initiating the biosynthesis of *O*-specific lipopolysaccharide and enterobacterial common antigen in *Escherichia coli*, *Microbiology 148*, 571−582.
15. Lloyd, A. J., Brandish, P. E., Gilbey, A. M., and Bugg, T. D. (2004) Phospho-*N*-acetyl-muramyl-pentapeptide translocase from *Escherichia coli*: catalytic role of conserved aspartic acid residues, *J. Bacteriol. 186*, 1747−1757.
16. Tamura, G. (1982) *Tunicamycins* (Tamura, G., Ed.) pp 10−31, Japan Scientific Press, Tokyo.
17. Tkacz, J. S. (1983) Tunicamycin and Related Antibiotics, in *Antibiotics VI* (Hohn, F. E., Ed.) pp 255−278, Springer-Verlag, Berlin.
18. Tsvetanova, B. C., Kiemle, D. J., and Price, N. P. J. (2002) Biosynthesis of tunicamycin and metabolic origin of the 11-carbon dialdose sugar, tunicamine, *J. Biol. Chem. 277*, 35289−35296.

19. Tsvetanova, B. C., and Price, N. P. J. (2001) Liquid chromatography-electrospray mass spectrometry of tunicamycin-type antibiotics, *Anal. Biochem. 289*, 147−156.

20. Heydanek, M. G., Jr., Struve, W. G., and Neuhaus, F. C. (1969) On the initial stage in peptidoglycan synthesis. 3. Kinetics and uncoupling of phospho-*N*-acetylmuramyl-pentapeptide translocase (uridine 5′-phosphate), *Biochemistry 8*, 1214−1221.

21. Xu L., and Price, N. P. (2004) Stereoselective synthesis of chirally deuterated (*S*)-D-(6-²H₁)glucose, *Carbohydr. Res. 339*, 1173−1178.

22. Momany, F. A., and Willett, J. L. (2000) Computational studies on carbohydrates: in vacuo studies using a revised AMBER force field, AMB99C, designed for α-(1→4) linkages, *Carbohydr. Res. 326*, 194−209.

23. Momany, F. A., and Willett, J. L. (2002) Molecular dynamics calculations on amylose fragments. I. Glass transition temperatures of maltodecaose at 1, 5, 10, and 15.8% hydration, *Biopolymers 63*, 99−110.

24. Parallel Quantum Solutions, 2013 Green Acres, Suite A, Fayetteville, AR.

25. Craik, D. J., Gosper, J. J., and Culvenor, C. C. J. (1989) Unambiguous stereochemical assignment of the glycosidic linkages of corynetoxin by ¹H NMR, *Aust. J. Chem. 42*, 541−547.

26. Perlman, M. E., Davis, D. G., Gabel, S. A., and London, R. E. (1990) Uridine diphospho sugars and related hexose phosphates in the liver of hexosamine-treated rats: identification using 31P-[1H] two-dimensional NMR with HOHAHA relay, *Biochemistry 29*, 4318−4325.

27. Murazumi, N., Yamamori, S., Araki, Y., and Ito, E. (1979) Anomeric configuration of *N*-acetylglucosaminyl phosphoryl undecaprenols formed in *Bacillus cereus* membranes, *J. Biol. Chem. 254*, 11791−11803.

28. Myers, A. G., Gin, D. Y., and Rogers, D. H. (1994) Synthetic studies of the tunicamycin antibiotics. Preparation of (+)-tunicaminyluracil, (+)-tunicamycin-V, and 5′-epi-tunicamycin-V, *J. Am. Chem. Soc. 116*, 4691−4118.

29. Inukai, M., Isono, F., and Takatsuki, A. (1993) Selective inhibition of the bacterial translocase reaction in peptidoglycan synthesis by mureidomycins, *Antimicrob. Agents Chemother. 37*, 980−983.

30. Muroi, M., Kimura, K., Osada, H., Inukai, M., and Takatsuki, A. (1997) Liposidomycin B inhibits in vitro formation of polyprenyl (pyro)phosphate *N*-acetylglucosamine, an intermediate in glycoconjugate biosynthesis, *J. Antibiot. 50*, 103−104.

31. Howard, N. I., and Bugg, T. D. H. (2003) Synthesis and activity of 5′-uridinyl dipeptide analogues mimicking the amino terminal peptide chain of nucleoside antibiotic mureidomycin A, *Bioorg. Med. Chem. 11*, 3083−3099.

32. Dini, C., Didier-Laurent, S., Drochon, N., Feteanu, S., Guillot, J. C., Monti, F., Uridat, E., Zhang, J., and Aszodi, J. (2002) Synthesis of sub-micromolar inhibitors of MraY by exploring the region originally occupied by the diazepanone ring in the liposidomycin structure, *Bioorg. Med. Chem. Lett. 12*, 1209−1213.

33. Dini, C., Drochon, N., Feteanu, S., Guillot, J. C., Peixoto, C., and Aszodi, J. (2001) Synthesis of analogues of the *O*-beta-D-ribofuranosyl nucleoside moiety of liposidomycins. Part 1: contribution of the amino group and the uracil moiety upon the inhibition of MraY, *Bioorg. Med. Chem. Lett. 11*, 529−531.

34. Taga, T., Miwa, Y., and Min, Z. (1997) α,β-trehalose monohydrate, *Acta Crystallogr. C53*, 234−236.